Cao *et al. Alzheimer's Research & Therapy* (2025) 17:108
https://doi.org/10.1186/s13195-025-01757-z

Alzheimer's Research & Therapy

RESEARCH Open Access

Shared genetic architecture between leukocyte telomere length and Alzheimer's disease

Zhi Cao[1,2†], Qilong Tan[3†], Hongxi Yang[4] and Chenjie Xu[2*]

Abstract

Background Epidemiological and clinical studies have reported an association between leukocyte telomere length (LTL) and Alzheimer's disease (AD). However, genetic association between the two phenotypes remains largely unknown. We aimed to elucidate the potential shared genetic architecture between LTL and AD.

Methods Summary statistics from genome-wide association studies were obtained from large-scale biobank in European-ancestry populations for LTL ($N = 472{,}174$) and AD (71,880 cases, 383,378 controls). We examined the global and local genetic correlation between LTL and AD using linkage-disequilibrium score regression and ρ-HESS. We applied the bivariate causal mixture model (MiXeR) to calculate the number of shared genetic causal variants, and the conditional/conjunctional false discovery rate (condFDR/conjFDR) framework to identify specific shared loci between LTL and AD. Bidirectional two-sample Mendelian randomization (MR) were used to explore the causal associations between LTL and AD.

Results We detected a significant genetic correlation between LTL and AD ($r_g = -0.168$). Partitioning the whole genome into 1703 almost independent regions, we observed a significant local genetic correlation for LTL and AD at 19q13.32. MiXeR estimated a total of 360 variants affecting LTL, of which 16 was estimated to influence AD. The condFDR revealed an essential genetic enrichment in LTL conditional on associations with AD, and vice versa. We next identified 8 shared genomic loci between LTL and AD using conjFDR method, of which 4 are novel loci for both the phenotypes. Moreover, 3 shared loci were identified as eQTLs (rs3098168, rs4780338 and rs2680702). All shared loci mapped a subset of 48 credible genes, including *USP8*, *DEXI* and *APOE*. Gene-set analysis identified 18 putative gene sets enriched with the genes mapped to the shared loci. MR analysis suggested that genetically determined AD was causally associated with LTL.

Conclusion Our study identified specific shared loci between LTL and AD, providing new insights for polygenic overlap and molecular mechanisms, and highlighting new opportunities for future experimental validation.

Keywords Leukocyte telomere length, Alzheimer's disease, Genetic architecture

†Zhi Cao and Qilong Tan contributed equally to this work.

*Correspondence:
Chenjie Xu
xuchenjie@hznu.edu.cn
[1]Department of Psychiatry, Sir Run-Run Shaw Hospital, Zhejiang University School of Medicine, Hangzhou, China
[2]School of Public Health, Hangzhou Normal University, NO.2318, Yuhangtang Road, Yuhang District, Hangzhou 311121, China
[3]School of Public Health, Zhejiang University School of Medicine, Hangzhou, China
[4]Department of Bioinformatics, School of Basic Medical Sciences, Tianjin Medical University, Tianjin, China

Introduction

Telomeres are protein-DNA complexes at the ends of chromosome that mitigate loss of coding DNA, since chromosomes are shortened with each cell division [1]. There has been much interest in a shorter leukocyte telomere length (LTL) as a biomarker of older biological age [2]. Telomeres have been considered potent drivers of genome stability, playing an important role in neuroplasticity to oxidative stress [3]. As oxidative stress is increased in older individuals, these mechanisms could be related to telomere shortening and aging manifestations such as cognitive disorders [4] A growing body of epidemiological and clinical studies have reported the associations between LTL and aging-related disorders, such as Alzheimer's disease (AD) [5, 6, 7]. However, it remains unclear about shared genetic etiology and causal relationship between them.

The genetic architectures of both LTL [8] and AD [9, 10] are highly polygenic, implying numerous genetic variants with small effects synthetically contributing to the phenotypes. Two large genome-wide association study (GWAS) meta-analysis of AD has identified 29 and 38 genome-wide significant loci [9, 10], which mapped genes are highly expressed in immune-related tissues and enriched for amyloid precursor proteins degradation pathways [9]. It has been difficult to determine genetic loci related to LTL until the recent well-powered GWASs of LTL from the UK Biobank with 472,174 participants, which identified 138 genetic loci and accounted for common variant LTL heritability of ~8.1% [8]. Despite the phenotypic overlap suggesting genetic pleiotropy, genetic overlap for LTL and AD remains elusive. Of note, these genetic data enable us to elucidate shared and distinct genetic architecture between LTL and AD, which can broaden our new insight into molecular mechanisms.

The aim of the present study was therefore to perform a comprehensive cross-trait GWAS analysis to examine the genetic overlap and the causal association between LTL and AD. Such analyses have several analytic aspects. First, a genetic correlation analysis that traditionally quantifies the average sharing of genetic effect between two traits was used to estimate global and local genetic correlation by linkage-disequilibrium score regression (LDSC). Next, we applied the bivariate causal mixture model (MiXeR) [11] and the conditional/conjunctional false discovery rate (cond/conjFDR) [12] method for large-scale GWASs of LTL and AD in order to (1) estimate the total number of shared genetic causal variants, (2) identify individual loci driving the phenotypic overlap between LTL and AD, and (3) leverage polygenic overlap to boost statistical power to identify novel loci related to LTL or AD. The MiXeR and cond/conjFDR framework have been extensively used in recent years to improve discovery power for identification of genomic loci and to determine shared genomic loci among a wide range of polygenic phenotypes, by leveraging the combined power of two GWAS regardless of the presence of a genetic correlation [13, 14, 15, 16, 17]. Finally, we conducted a bidirectional two-sample Mendelian randomization (MR) analysis to infer putative causal relationships between LTL and AD. To the best of our knowledge, no cross-trait GWAS analysis has been performed to investigate comprehensively the shared and distinct etiology underlying LTL and AD. The overall study design is shown in Fig. 1.

Methods

GWAS data and quality control

We acquired summary statistics for LTL from the UK Biobank, which consisted of 472,174 well-characterized participants who measured LTL by quantitative Polymerase Chain Reaction (PCR) assay [8]. GWAS summary statistics for AD were acquired from the Psychiatric Genomics Consortium (PGC), which comprised 71,880 AD cases, 383,378 controls [9]. All participants were of European ancestry. Detailed description of each sample is provided in the original publications [8, 9].

For the two phenotypes, quality control were undertaken stringently: removed duplicated SNPs or those not included in the 1000 Genomes Project or whose alleles did not match those there; excluded non-biallelic SNPs and those with strand-ambiguous alleles; excluded SNPs that were located within the region of major histocompatibility complex (chr6: 28.5–33.5 Mb) as its complex LD structure [18]; excluded SNPs without rsID label; excluded SNPs with minor allele frequency (MAF) < 0.01.

Statistical analyses

Global and local genetic correlation analysis

To elucidate the genetic architecture between LTL and AD, a global genetic correlation analysis was undertaken by linkage disequilibrium score regression (LDSC) [18]. It can be estimated using GWAS summary statistics through an algorithm implemented in LDSC software [18, 19]. LDSC analyses were performed with and without a constrained intercept, since constraining single trait heritability intercepts can improve the accuracy of estimates when there are sample overlap and minimal population stratification [18].

Global genetic correlations calculated by LDSC are based on aggregated information across whole genome variants. Even though the global genetic correlation is extremely small between two phenotypes, there might be specific regions in the genome contributing to both phenotypes. Nevertheless, we further assessed pairwise local genetic correlations for LTL and AD using ρ-HESS [20], an algorithm that partitions the genome-wide genetic sharing across 1703 nearly independent linkage disequilibrium (LD) regions of 1.5 Mb and precisely assesses the

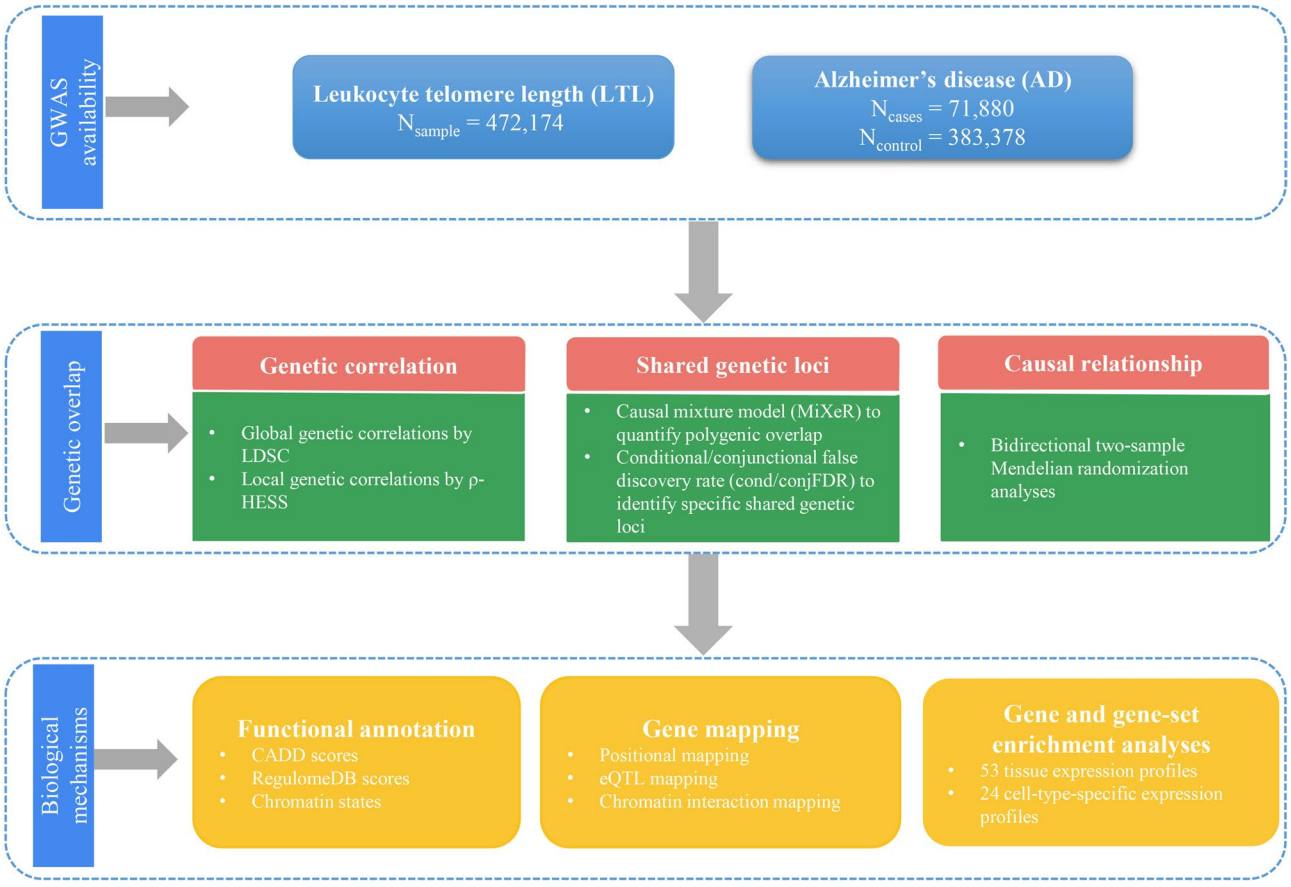

Fig. 1 Outline of the current study

genetic correlation between two phenotypes because of genetic variation restricted to these genomic regions.

MiXeR

To quantify polygenic overlap between LTL and AD, we applied the MiXeR statistical tool [11], which quantifies the number of phenotype-specific and shared causal variants between two phenotypes, and the results are displaying as a Venn diagram. "Causal" refers to the cause of the statistical association and not necessarily the biological cause of the conditions studied. MiXeR includes univariate estimation of the number of phenotype-influencing loci for each phenotype of interest and bivariate estimation of genome-wide genetic overlap between two phenotypes. We calculated the Dice coefficient (DC) index (polygenic overlap measure in the 0–100% scale) and genetic correlation between two phenotypes. Univariate and bivariate estimation and standard errors were computed by 20 iterations using 2 million randomly selected SNPs for each iteration, and then random pruning at an LD threshold of $r^2 = 0.8$ is conducted. Model fit was based on GWAS z-scores.

CondFDR/conjFDR

To provide a visual representation and assess cross-traits polygenic enrichment between LTL and AD, conditional quantile–quantile (Q-Q) plots were constructed [21]. The conditional Q-Q plots compare the association with one phenotype (e.g. LTL) within SNPs strata determined by the strength of association with a secondary phenotype (e.g. AD). Enrichment for overlapping signals exists for a given phenotype if the degree of leftward deflection from the expected null line increases with increasing association significance in the second phenotype [21].

Then, we employed the condFDR/conjFDR method [12], which using polygenic overlap between two traits to improve statistical power to determine loci related to a single phenotype (condFDR) and loci jointly related to two phenotypes (conjFDR), thus complementing the genome-wide genetic overlap observed with MiXeR. This framework extends the standard FDR approcach and builds on an empirical Bayesian framework to control type 1 errors by using all *p*-values from GWAS results for both phenotypes, and by re-ranking the test statistics for a primary phenotype conditioned on a secondary phenotype.

The conjFDR approach, on the basis of the condFDR, was also performed to test which loci showed evidence of association with both phenotypes. The conjFDR statistic is defined as the maximum of the two mutual condFDR values and is a conservative estimate of the posterior probability that an SNP has no association with either phenotype, given that the *P* values for that SNP in both the primary and conditional phenotypes are lower than the observed *P* values. Thus, the conjFDR approach can identify loci jointly associated with these two phenotypes. The FDR significance cutoffs were 0.05 for conjFDR and 0.01 for condFDR in accordance with previous studies [22, 23, 24].

Definition of genomic loci

As described previously [25], genomic risk loci were defined within Functional Mapping and Annotation (FUMA; https://fuma.ctglab.nl). First, we identified independent significant SNPs as SNPs that were independent from each other at $r^2 < 0.60$ and that reached a condFDR < 0.01 or conjFDR < 0.05 in the respective condFDR or conjFDR analysis. Those independent significant SNPs were further clumped at $r^2 = 0.1$ to define lead SNPs. Independent significant SNPs that were in LD with the same lead SNPs ($r^2 > 0.1$) and LD blocks closer than 250 kb were merged into a single locus. Candidate SNPs were defined as SNPs in the genomic loci with a condFDR or conjFDR value < 0.10 having an LD $r^2 \geq 0.6$ with one of the independent significant SNPs. In line with prior evidence [26], the candidate SNP cond/conjFDR thresholds were lowered to maximize the probability that putative traits-influencing SNPs were captured within each locus. The directional effects of the loci shared between LTL and AD were assessed by comparing the z-scores of their lead SNPs. A locus that was not physically overlapping with findings from the original GWASs [8, 9] or NHGRI-EBI GWAS Catalog [27] (last accessed on February 20, 2023) was considered as novel.

Functional annotation, gene mapping, and gene-set analyses

All candidate SNPs were functionally annotated using FUMA platform. Functional consequences of SNPs on genes were acquired by running ANNOVAR [28] gene-based annotation using Ensembl genes. Enrichments of candidate SNPs in each annotation were tested by Fisher's exact test by comparing them with the annotations of all SNPs analyzed in the cond/conjFDR. We annotated SNPs based on functional categories, CADD scores, RegulomeDB scores and chromatin states. CADD score [29] was annotated for each SNP to determine the deleteriousness of SNPs, a CADD score above 12.37 is the threshold to be potentially pathogenic. The RegulomeDB score [30] is a categorical score based on information from eQTLs and chromatin marks, ranging from 1a to 7, with lower scores indicating an increased likelihood of having a regulatory function. Chromatin state [31] suggests the accessibility of genomic regions with 15 categorical states predicted by ChromHMM based on 5 chromatin marks for 127 tissue/cell types obtained from Roadmap.

All candidate SNPs obtained by the cond/conjFDR were mapped to genes using three strategies [25]: (1) positional mapping to align SNPs to genes based on their physical proximity, (2) expression quantitative trait locus (eQTL) mapping to match cis-eQTL SNPs to genes whose expression is associated with allelic variation at the SNP level, and (3) chromatin interaction mapping to link SNPs to genes based on three-dimensional DNA–DNA interactions between each SNP's genomic region and nearby or distant genes. Credible genes were mapped by at least 2 strategies above.

On each set of mapped genes, we performed gene-set enrichment analysis within the Gene Ontology (GO) classification system [32]. Additionally, genotype tissue expression (GTEx) data resource [33] was applied to assess gene expression and look at the eQTL functionality of likely regulatory SNPs in the shared loci between LTL and AD. All reported *P* values were corrected for multiple testing by the false discovery rate (FDR)approach.

Bidirectional two-sample MR analyses

To further investigate the causal association between LTL and AD, a two-sample MR approach was employed [34]. Genetic instruments were sourced from summary statistics by thresholding at a significance level of 5×10^{-8} and clumping according to $r^2 < 0.01$ using a 1000 Genomes European population reference. To validate whether the instrumental variable (IV) set is strong (F-statistics > 10), we estimated the F-statistics for each phenotype [35]. For each exposure, the primary MR analysis was performed by using the inverse-variance weighting (IVW) under a multiplicative random-effects model [36]. In addition, a series of sensitivity analyses were undertaken to verify the pleiotropy in the causal estimates. The potential presence of horizontal pleiotropy was evaluated by MR-Egger regression based on its intercept term, where deviation from zero ($P < 0.05$) was considered to provide evidence for the presence of directional pleiotropic bias [37]. We also performed the weighted-median [38], weighted-mode [39] methods in the sensitivity analyses on the basis of different assumptions. The leave-one-SNP-out analysis was conducted to confirm whether the causal association was obviously driven by a single SNP (a *P* value of < 0.05 was regarded as an outlier). The presence of pleiotropy was also estimated using MR-PRESSO, which detects and corrects the effects from outliers, yielding causal estimates that are robust to heterogeneity [40]. To address the issue of sample overlap between LTL and AD datasets, we first evaluated the bias and type 1 error rate for

sample overlap based on an online calculator (https://sb452.shinyapps.io/overlap/) [35], then we used the summary statistics from Wightman et al. [10] that excluded UK Biobank participants to replicate our findings. All analyses were performed using the TwoSampleMR and MR-PRESSO packages [40, 41] in R software.

Results

Genetic correlations between LTL and AD

We found a significant overall genetic correlation between LTL and AD using unconstrained LDSC (r_g = -0.168, P = 0.017) (Supplementary Table S1). We further constrained the intercepts of genetic covariance estimates to zero, through which LDSC could indicate greater power with slightly decreased standard errors. A strongly negative genetic correlation was observed for LTL and AD (r_g = -0.139, $P = 1.71 \times 10^{-5}$). Motivated by the significant overall genetic correlation, we further explored the local genetic correlation using ρ-HESS (Fig. 2) [20]. A strong local signal was only observed at 19q13.32 (chr19: 44744000–46103000) ($P = 8.45 \times 10^{-8}$) (Supplementary Figure S1).

Polygenic overlap pattern

Univariate MiXeR estimated that LTL was approximately 14 times more polygenic relative to AD, with 360 variants estimated to influence LTL compared to 25 in AD. Detail information of heritability, polygenicity, discoverability and power analyses are described in the Supplementary Table S2. Bivariate MiXeR demonstrated moderate polygenic overlap between LTL and AD, beyond that captured by genetic correlation (Supplementary Figure S2). Of a total of 360 variants estimated to influence LTL, 16 (SD = 4, 4.4%) was estimated to influence AD (Dice coefficient = 8%) (Supplementary Table S2). Consistent with genetic correlation by LDSC, bivariate MiXeR also estimated a moderately negative genetic correlation (r_g = -0.13). The stratified conditional QQ plots showed SNP enrichment for LTL as a function of their associations with AD and vice versa (Supplementary Figure S2c and 2d), suggesting the existence of polygenic overlap.

Shared genetic loci

To improve the discovery of genetic variants, we applied condFDR to perform the cross-trait enrichment between LTL and AD and reranked LTL SNPs conditionally on its association with AD and vice versa (Supplementary Figure S3). At condFDR < 0.01, we identified 263 loci associated with LTL conditional on its association with AD (Supplementary Table S3 and Figure S4). The reverse condFDR analyses identified 122 loci associated with AD, conditional on LTL (Supplementary Table S4 and Figure S5).

ConjFDR method was then used to identify the shared genetic loci between LTL and AD. At conjFDR < 0.05, a total of 8 distinct genomic loci were jointly associated with LTL and AD, in which 6 were novel for LTL and 4 for AD (Fig. 3; Table 1, Supplementary Tables S5 and S6). Altogether, we identified 4 novel loci in both phenotypes. Then, we assessed the directionality of allelic effects of the shared lead SNPs between the phenotypes by examining their z-scores. There was a pattern of mixed effect directions of the shared SNPs between LTL and AD (Table 1). We discovered the same effect direction of 62.5% of SNPs shared. For the independent significant SNPs within locus and their tagged SNPs, a summary of previous SNP-phenotype associations with other phenotypes are listed in Supplementary Table S7.

Biological insights for the shared loci

Functional annotation of all candidate SNPs in the loci shared between LTL and AD phenotypes demonstrated that these were mostly intronic (69.74%) and intergenic (13.3%), only 1.49% in exons (Fig. 4). The distribution of minimum chromatin state shows that 99.3% of the SNPs in the shared loci are in open chromatin state regions,

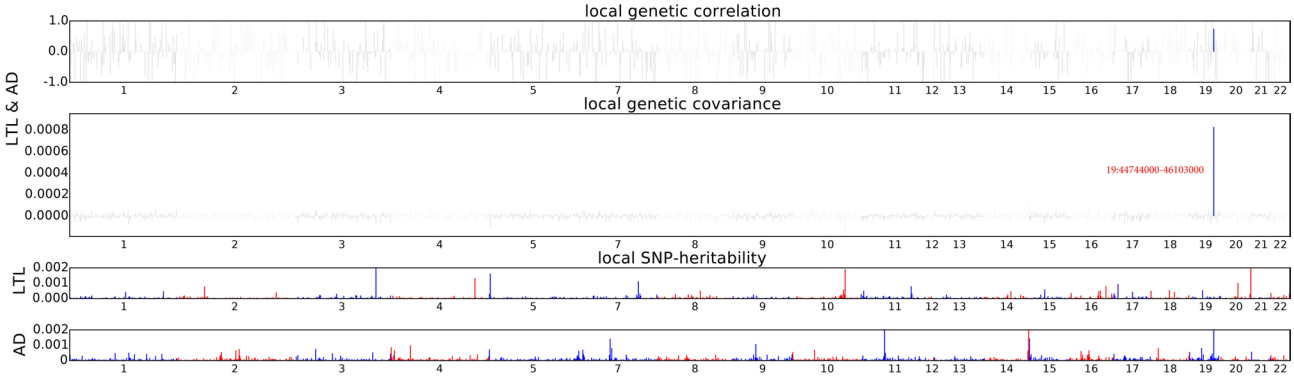

Fig. 2 Local genetic correlation between LTL and AD. Manhattan plot showing the estimates of local genetic correlation, genetic covariance, and SNP heritability between LTL and AD overall. Blue bars represent loci showing significant local genetic correlation after multiple testing adjustment ($p < 0.05/1{,}703$)

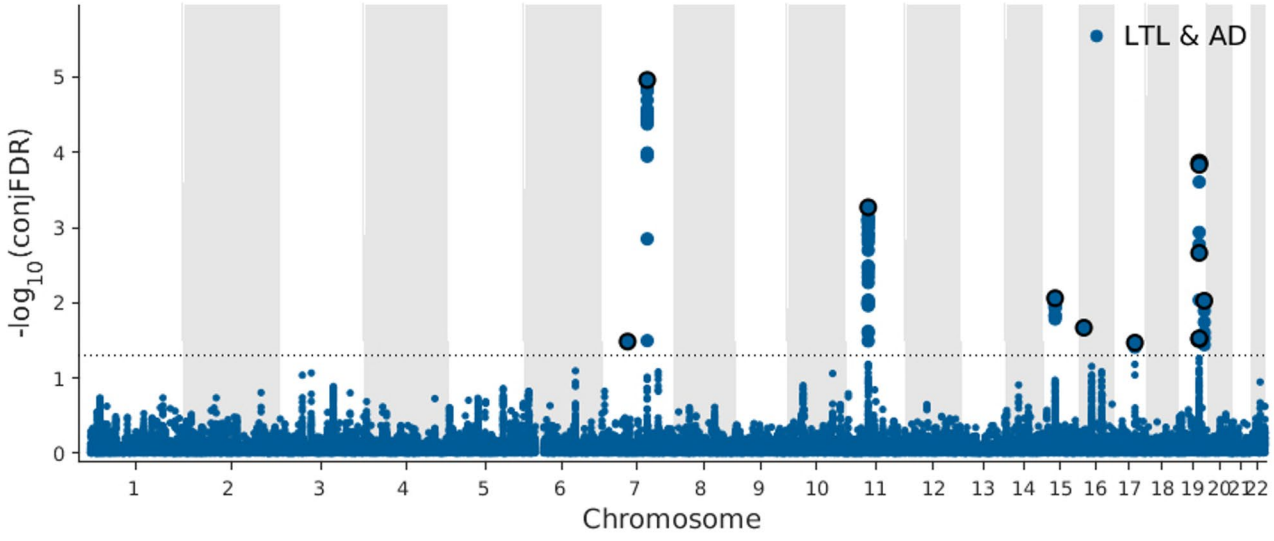

Fig. 3 Common genetic variants jointly associated with LTL and AD at conjFDR < 0.05. Manhattan plots showing the–log10 transformed conjunctional FDR values for LTL and AD for each SNP (y-axis) against chromosomal position (x-axis). The dotted line represents the conjFDR threshold for significant association < 0.05. Black outlined circles represent independent lead SNPs. Details for genomic loci and candidate single-nucleotide variants are provided in Table 1 and Supplementary Table S5

making them more accessible to DNA regulatory elements. We mapped 174 protein-coding genes to candidate SNPs for LTL and AD, in which 48 credible mapped genes by at least two gene-mapping strategies (Supplementary Table S8). Credible genes of shared loci showed a high expression in the brain and whole blood tissues (Fig. 5). Gene-set analyses revealed 18 significantly associated biological and cellular processes with the genes mapped to the shared loci, including "very low density lipoprotein particle clearance", "cholesterol efflux", "regulation of sterol transport", "phospholipid efflux" (Supplementary Table S9). All the novel shared loci identified by the conjFDR were represented by 4 unique lead SNPs, of which 3 (rs3098168, rs4780338 and rs2680702) were identified as eQTLs for 20 unique genes within 28 different tissues in the GTEx database (Supplementary Table S10).

Bidirectional MR analyses

We applied a two-sample MR analysis to test the causal relationship between LTL and AD. In the forward MR analysis, the genetic instrument for LTL consisted of 125 independent significant SNPs (Supplementary Table S11). Collectively, these SNPs explained 3.0% of the variance in LTL in this sample and could be considered a strong instrument (F statistic = 118.7). In the primary MR analysis (IVW), we found that genetically determined LTL was not causally associated with risk of AD (OR = 0.99, 95% CI: 0.91–1.09, $P = 0.873$) (Fig. 6 and Supplementary Figure S6). The direction of effect was consistent with MR-PRESSO, weighted median and MR-Egger, although weighted mode regression had a marginal *P* value. The intercept of MR-Egger regression test did not identify any horizontal pleiotropy (β = 0.0018, $P = 0.42$). In the reverse MR analysis, using 33 SNPs robustly and independently associated with AD as instrument variables (Supplementary Table S12), MR provided strong causal evidence that AD shortened the LTL (β = 0.070, 95% CI = 0.030–0.109, $P = 5.3 \times 10^{-4}$). The intercept of MR-Egger regression test did not identify any horizontal pleiotropy (β = -0.0013, $P = 0.11$). In the sensitivity analysis, the MR-PRESSO test detected 1 potential outlier, with the results being stable after outlier correction (β = 0.072, 95% CI = 0.043–0.101, $P = 2.0 \times 10^{-5}$). The estimates were similar in size in weighted median (β = 0.070; 95% CI, 0.019–0.120; $P = 0.007$) and MR Egger (β = 0.105; 95% CI, 0.048–0.163; $P = 0.001$), supporting a strong effect of AD on LTL (Fig. 6 and Supplementary Figure S6). Moreover, we found the type 1 error rate due to sample overlap between LTL and AD was well controlled under 0.05, indicating that sample overlap might not significantly bias the causal association. We used another GWAS summary statistics of AD excluding the UK Biobank sample, suggesting the consistent MR findings (Supplemental Table S13).

Discussion

By leveraging large GWAS summary datasets, our study provided insights into the polygenic architecture and overlap between aging-related phenotype. Using the novel MiXeR tool, our findings showed that 8% of causal variants of LTL influence AD, despite a mild part of the polygenic architecture. Subsequently, we identified 8 genomic loci jointly associated with LTL and AD using a condFDR/conjFDR approach, of which half of loci

Table 1 Novel loci jointly associated with LTL and AD at conjfdr < 0.05

Locus	Lead SNP	CHR	Position	A1/A2	Nearest Gene	Functional Category	conjFDR	LTL			AD			Cor_Eff[b]
								Z-score	*P* value	Novel[a]	Z-score	*P* value	Novel[a]	
1	rs17552904	7	50,318,308	T/G	AC020743.4	Intergenic	3.27E-02	3.705	2.11E-04	Yes	4.031	5.56E-05	Yes	+
2	rs12705073	7	99,774,122	C/T	GPC2	Intronic	1.09E-05	-5.575	2.47E-08	No	-5.840	5.22E-09	No	+
3	rs10437655	11	47,391,948	A/G	SPI1	Intronic	5.38E-04	-5.633	1.77E-08	No	4.865	1.14E-06	No	-
4	rs3098168	15	50,751,050	C/T	USP8	Intronic	8.69E-03	4.120	3.78E-05	Yes	-4.259	2.06E-05	Yes	-
5	rs4780338	16	11,031,156	T/C	DEXI	Intronic	2.15E-02	3.890	1.00E-04	Yes	4.038	5.39E-05	Yes	+
6	rs2680702	17	56,431,549	G/A	RNF43	ncRNA_intronic	3.39E-02	4.194	2.75E-05	Yes	-3.919	8.88E-05	Yes	-
7	rs1065853	19	45,413,233	T/G	APOE	Downstream	1.37E-04	-5.086	3.65E-07	Yes	-6.984	2.88E-12	No	+
8	rs1761452	19	54,815,366	T/C	AC008984.7	ncRNA_intronic	9.40E-03	-4.120	3.78E-05	Yes	-4.241	2.23E-05	No	+

Abbreviations: A1, allele 1 (effect allele); A2, allele 2 (noneffect allele); conjFDR, conjunctional false discovery rate; AD, Alzheimer's disease; CHR, chromosome; Cor_Eff, concordancy of association directions between 2 traits; LTL, leukocyte telomere length; SNP, single nucleotide polymorphism

a Whether a locus was novel for 2 traits, according to the original GWAS or GWAS Catalog

b The directionality of allelic associations with both phenotypes in discovery data sets using z scores is shown here. + Indicates the same direction and -, the opposite direction

have not been reported before for both the phenotypes. Moreover, we annotated these specific shared loci and identified a subset of 48 credible genes and many eQTLs for multiple tissues. Finally, MR analysis suggested that genetically determined AD was causally associated with LTL. Our findings provide new insight into the molecular mechanisms shared between LTL and AD.

Our findings suggested a light genetic correlation between LTL and AD, which may be partly attribute to the relatively small number of causal variants related to AD (univariate MiXeR estimated 25 causal variants) compared to LTL (univariate MiXeR estimated 360 causal variants), or the mixed direction of effects among the variants shared across the two phenotypes (the shared SNPs of concordant effect direction of was 62.5%). These findings contribute to accumulatively numerous evidence suggesting extensive polygenic overlap across a range of complex, brain-related phenotypes, with mixed directions of effect and minimal genetic correlation [14, 42]. Firstly, local genetic correlations using ρ-HESS [20] revealed a strong local signal at 19q13.32, this genomic region harbors protein coding *MARK4*, a member of the microtubule affinity-regulating kinase family [43]. *MARK4* isoform is primarily found in brain tissue, leading to microtubule destabilization in neuronal cells and also tau-protein phosphorylation seen in AD [44]. Secondly, the conjFDR statistical approach used in our study, which enables the identification of genomic loci jointly affecting both phenotypes, singled out 8 specific loci shared between LTL and AD, further dissecting their polygenic overlap. When boosting the power from the combined samples, condFDR identified 263 loci in LTL conditioned on AD and 122 loci in AD conditioned on LTL. These discovered loci can help to explain more of the heritability underlying LTL and AD traits. Through leveraging the cross-trait enrichment to improve statistical power, this enabled the identification of novel risk loci in LTL and AD, these findings warrant future validation [12, 45].

We functionally annotated all shared loci to explore putative biological mechanisms linking the polygenic overlap and phenotypic associations observed between LTL and AD. Most of the SNPs identified in the shared loci between LTL and AD by the conjFDR analysis, are in intronic regions that are likely to impact expression/regulation, and are not predicted to be highly deleterious based on CADD scores. In the conjFDR analysis, we found that 4 of 8 shared loci were both novel for LTL and AD, including rs17552904, rs3098168, rs4780338 and rs2680702. The lead SNP at the locus (rs3098168) was identified as an eQTL for *USP8* (15q21.2) in the GTEx database and significantly regulates the expression of the gene in several human brain regions [46]. *USP8* regulates the ubiquitination, trafficking, and lysosomal degradation

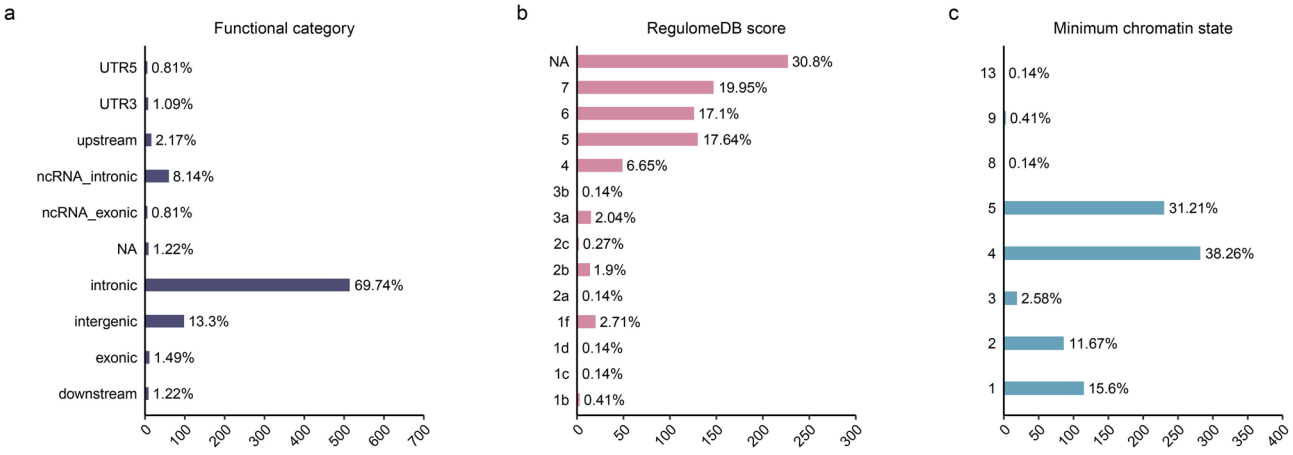

Fig. 4 Distribution of the annotation for all candidate SNPs jointly associated between LTL and AD. (**a**) Distribution of functional consequences of SNPs in the shared genomic risk loci. (**b**) Distribution of RegulomeDB scores for SNPs in the shared genomic loci, with a low score indicating a higher likelihood of having a regulatory function. (**c**) The minimum chromatin state across 127 tissue and cell types for SNPs in shared genomic loci, with lower states indicating higher accessibility and states 1–7 referring to open chromatin states

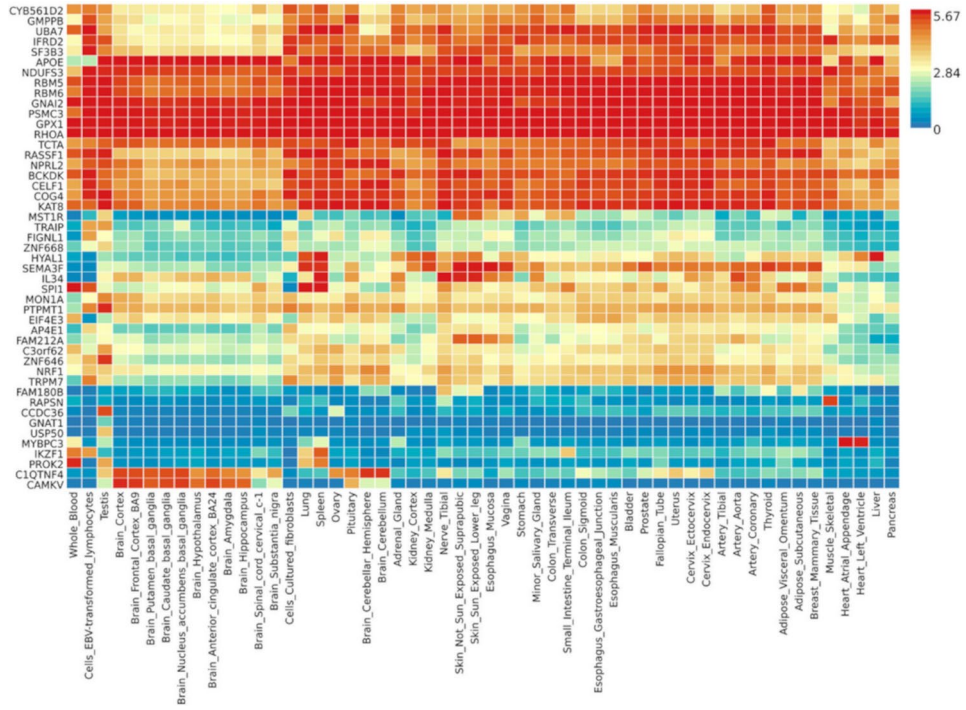

Fig. 5 Spatiotemporal gene expression of credible genes of shared loci between LTL and AD. Among all mapping candidate SNPs of the shared loci between LTL and AD, 48 credible genes were mapped by at least 2 strategies: positional mapping, expression quantitative trait locus mapping, and chromatin interaction mapping. The gene expression data were acquired from the Genotype Tissue Expression (GTEx) v8 resource and the figure was generated using the GENE2FUNC procedure of FUMA. Gene expression was based on data from 948 individuals and is presented as the averaged log2 transformed expression per tissue for each gene. Darker red means higher gene expression compared to a darker blue color

of several plasma membrane proteins, and its mutation is regarded as be potential therapeutic targets for Cushing Disease [47]. The lead SNP at the locus (rs4780338) was also identified as an eQTL for *DEXI* (16p13.13) in the GTEx database, and is associated with type 1 diabetes [48] and asthma [49]. Moreover, we determined a subset of 48 unique credible genes that map to specific identified shared loci based on three gene-mapping strategies. For instance, *APOE* gene is regarded as a strongest genetic risk factor for AD [50], interestingly, our cross-traits analysis revealed *APOE* might also be a significant genomic loci of LTL. A prior study showed that shortened LTL may be associated with the *ApoE4* homozygote in AD patients [51]. Notably, the MR analysis in our

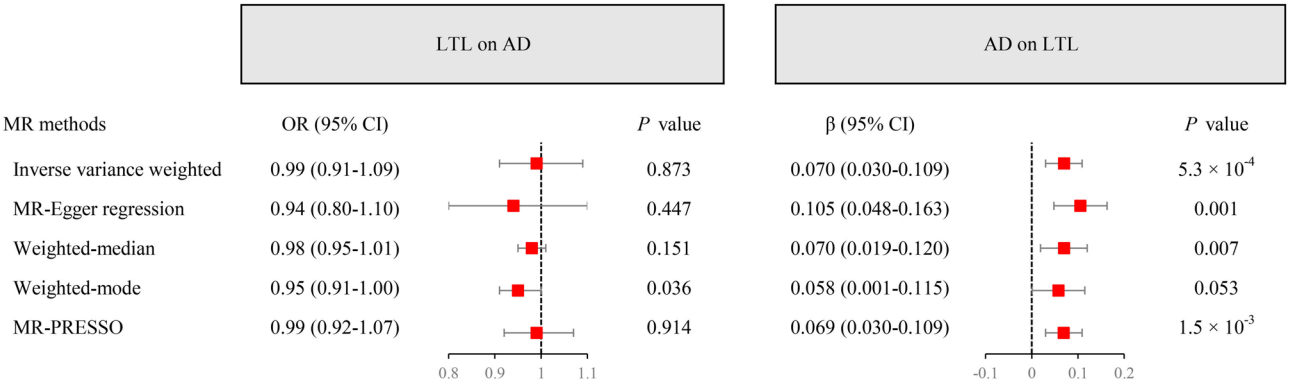

Fig. 6 Bidirectional MR results for the relationship between LTL and AD

study showed that LTL was not causally associated with AD, whereas AD was causally related to shortened LTL. Previous evidence from observational studies have suggested an association between LTL and AD [6, 52]. As such, a relation between LTL and AD is well established, but the underlying causal association has been difficult to determine from clinical and epidemiological data. Our findings highlight that genetic risk variants for AD contribute to the variance in LTL. These findings provide further evidence for the strong association between AD and LTL, suggesting an essential shared genetic basis and neurobiological mechanisms.

There were limitations to the current study. This study was using European samples only, which limits the generalizability of these findings to other ancestral groups. It is important that more diverse samples and improved approaches for trans-ancestral analysis are used to broaden the applicability of genetic studies. Moreover, current approaches used in this study dependent on common variant from published GWAS summary statistics, thus, only the common variant data for LTL and AD were performed in our study. Consequently, some rare and structural variations important to the genetic architecture of these two phenotypes were not adequately taken into consideration.

Conclusion

In conclusion, the present study identified shared genetic architecture, beyond genetic correlation, between LTL and AD. We identified 8 shared loci and a subset of credible genes likely to play a role in the underlying genetic etiology of LTL and AD, which may represent novel drug targets and thus opportunities for personalized approaches to treatment. These findings have implications for substantially enhancing our understanding of molecular genetic basis between aging-related biomarker and diseases. Future experimental studies of the identified shared loci between the aging-related biomarker and diseases may provide new knowledge for molecular mechanisms, which can ultimately facilitate the development of AD drugs by identifying potential therapeutic targets.

Supplementary Information

The online version contains supplementary material available at https://doi.org/10.1186/s13195-025-01757-z.

Supplementary Material 1

Supplementary Material 2

Acknowledgements

We thank the research participants, employees and investigators of the Psychiatric Genetics Consortium and UK Biobank for genome-wide association study data.

Author contributions

ZC and QT contributed to this work equally. CX and ZC, QT were involved in the conception, design, and conduct of the study and the analysis and interpretation of the results. ZC and QT wrote the first draft of the manuscript, and all authors edited, reviewed, and approved the final version of the manuscript. ZC and QT analyzed the data and interpretated the results. CX and HY have made critical revision of the manuscript for important intellectual content. CX had full access to all the data in the study, and takes responsibility for the integrity of the data and the accuracy of the data analysis.

Funding

This work was supported by National Natural Science Foundation of China (grant number 72204071); Zhejiang Provincial Natural Science Foundation of China (grant number LY23G030005); Scientific Research Foundation for Scholars of HZNU (grant number 4265C50221204119).

Data availability

GWAS summary statistics used in this article were obtained from the UK Biobank (https://www.ukbiobank.ac.uk/) and the Psychiatric Genomics Consortium (https://www.med.unc.edu/pgc/). GTEx expression summary data are available from https://gtexportal.org/home/datasets. Gene information was obtained from the GeneCard database (v5.12.0 Build 702; https://www.genecards.org). NHGRI-EBI GWAS Catalog: ULGWAS summary statistics, https://www.ebi.ac.uk/gwas/downloads/summary-statistics.

Code availability

The codes for MiXeR and conditional and conjunctional FDR analyses are publicly available at https://github.com/precimed/mixer and https://github.com/precimed/pleiofdr/, respectively. Other methods used are as follows: LDSC: https://github.com/bulik/ldsc; ρ-HESS: https://github.com/bulik/ldsc. TwoSampleMR: https://mrcieu.github.io/TwoSampleMR/, FUMA (v1.4.0) GWAS platform: http://fuma.ctglab.nl/.

Declarations

Ethics approval and consent to participate
Not applicable.

Consent for publication
Not applicable.

Competing interests
The authors declare no competing interests.

Received: 7 November 2023 / Accepted: 7 May 2025
Published online: 17 May 2025

References

1. O'Sullivan RJ, Karlseder J. Telomeres: protecting chromosomes against genome instability. Nat Rev Mol Cell Biol. 2010;11(3):171–81.
2. López-Otín C, Blasco MA, Partridge L, Serrano M, Kroemer G. The hallmarks of aging. Cell. 2013;153(6):1194–217.
3. Spilsbury A, Miwa S, Attems J, Saretzki G. The role of telomerase protein TERT in Alzheimer's disease and in Tau-Related pathology in vitro. J Neurosci. 2015;35(4):1659–74.
4. Eitan E, Hutchison ER, Mattson MP. Telomere shortening in neurological disorders: an abundance of unanswered questions. Trends Neurosci. 2014;37(5):256–63.
5. Hackenhaar FS, Josefsson M, Adolfsson AN, Landfors M, Kauppi K, Hultdin M, Adolfsson R, Degerman S, Pudas S. Short leukocyte telomeres predict 25-year Alzheimer's disease incidence in non-APOE ε4-carriers. Alzheimers Res Ther. 2021;13(1):130.
6. Honig LS, Kang MS, Schupf N, Lee JH, Mayeux R. Association of shorter leukocyte telomere repeat length with dementia and mortality. Arch Neurol. 2012;69(10):1332–9.
7. Forero DA, Gonzalez-Giraldo Y, Lopez-Quintero C, Castro-Vega LJ, Barreto GE, Perry G. Meta-analysis of telomere length in Alzheimer's disease. Journals Gerontol Ser a-Biological Sci Med Sci. 2016;71(8):1069–73.
8. Codd V, Wang Q, Allara E, Musicha C, Kaptoge S, Stoma S, Jiang T, Hamby SE, Braund PS, Bountziouka V, et al. Polygenic basis and biomedical consequences of telomere length variation. Nat Genet. 2021;53(10):1425–33.
9. Jansen IE, Savage JE, Watanabe K, Bryois J, Williams DM, Steinberg S, Sealock J, Karlsson IK, Hägg S, Athanasiu L, et al. Genome-wide meta-analysis identifies new loci and functional pathways influencing Alzheimer's disease risk. Nat Genet. 2019;51(3):404–13.
10. Wightman DP, Jansen IE, Savage JE, Shadrin AA, Bahrami S, Holland D, Rongve A, Børte S, Winsvold BS, Drange OK, et al. A genome-wide association study with 1,126,563 individuals identifies new risk loci for Alzheimer's disease. Nat Genet. 2021;53(9):1276–82.
11. Frei O, Holland D, Smeland OB, Shadrin AA, Fan CC, Maeland S, O'Connell KS, Wang Y, Djurovic S, Thompson WK, et al. Bivariate causal mixture model quantifies polygenic overlap between complex traits beyond genetic correlation. Nat Commun. 2019;10(1):2417.
12. Smeland OB, Frei O, Shadrin A, O'Connell K, Fan CC, Bahrami S, Holland D, Djurovic S, Thompson WK, Dale AM, et al. Discovery of shared genomic loci using the conditional false discovery rate approach. Hum Genet. 2020;139(1):85–94.
13. Bahrami S, Shadrin A, Frei O, O'Connell KS, Bettella F, Krull F, Fan CC, Røssberg JI, Hindley G, Ueland T, et al. Genetic loci shared between major depression and intelligence with mixed directions of effect. Nat Hum Behav. 2021;5(6):795–801.
14. Bahrami S, Hindley G, Winsvold BS, O'Connell KS, Frei O, Shadrin A, Cheng W, Bettella F, Rødevand L, Odegaard KJ, et al. Dissecting the shared genetic basis of migraine and mental disorders using novel statistical tools. Brain. 2022;145(1):142–53.
15. Elvsåshagen T, Shadrin A, Frei O, van der Meer D, Bahrami S, Kumar VJ, Smeland O, Westlye LT, Andreassen OA, Kaufmann T. The genetic architecture of the human thalamus and its overlap with ten common brain disorders. Nat Commun. 2021;12(1):2909.
16. O'Connell KS, Frei O, Bahrami S, Smeland OB, Bettella F, Cheng W, Chu Y, Hindley G, Lin A, Shadrin A, et al. Characterizing the genetic overlap between psychiatric disorders and Sleep-Related phenotypes. Biol Psychiatry. 2021;90(9):621–31.
17. Cheng W, Frei O, van der Meer D, Wang Y, O'Connell KS, Chu Y, Bahrami S, Shadrin AA, Alnæs D, Hindley GFL, et al. Genetic association between schizophrenia and cortical brain surface area and thickness. JAMA Psychiatry. 2021;78(9):1020–30.
18. Bulik-Sullivan B, Finucane HK, Anttila V, Gusev A, Day FR, Loh PR, Duncan L, Perry JR, Patterson N, Robinson EB, et al. An atlas of genetic correlations across human diseases and traits. Nat Genet. 2015;47(11):1236–41.
19. Bulik-Sullivan BK, Loh PR, Finucane HK, Ripke S, Yang J, Patterson N, Daly MJ, Price AL, Neale BM. LD score regression distinguishes confounding from polygenicity in genome-wide association studies. Nat Genet. 2015;47(3):291–5.
20. Shi H, Mancuso N, Spendlove S, Pasaniuc B. Local genetic correlation gives insights into the shared genetic architecture of complex traits. Am J Hum Genet. 2017;101(5):737–51.
21. Adams MJ, Howard DM, Luciano M, Clarke TK, Davies G, Hill WD, Smith D, Deary IJ, Porteous DJ, McIntosh AM. Genetic stratification of depression by neuroticism: revisiting a diagnostic tradition. Psychol Med. 2020;50(15):2526–35.
22. Karch CM, Wen N, Fan CC, Yokoyama JS, Kouri N, Ross OA, Höglinger G, Müller U, Ferrari R, Hardy J, et al. Selective genetic overlap between amyotrophic lateral sclerosis and diseases of the frontotemporal dementia spectrum. JAMA Neurol. 2018;75(7):860–75.
23. Liu JZ, Hov JR, Folseraas T, Ellinghaus E, Rushbrook SM, Doncheva NT, Andreassen OA, Weersma RK, Weismüller TJ, Eksteen B, et al. Dense genotyping of immune-related disease regions identifies nine new risk loci for primary sclerosing cholangitis. Nat Genet. 2013;45(6):670–5.
24. Smeland OB, Frei O, Kauppi K, Hill WD, Li W, Wang Y, Krull F, Bettella F, Eriksen JA, Witoelar A, et al. Identification of genetic loci jointly influencing schizophrenia risk and the cognitive traits of Verbal-Numerical reasoning, reaction time, and general cognitive function. JAMA Psychiatry. 2017;74(10):1065–75.
25. Watanabe K, Taskesen E, van Bochoven A, Posthuma D. Functional mapping and annotation of genetic associations with FUMA. Nat Commun. 2017;8(1):1826.
26. Smeland OB, Shadrin A, Bahrami S, Broce I, Tesli M, Frei O, Wirgenes KV, O'Connell KS, Krull F, Bettella F, et al. Genome-wide association analysis of Parkinson's disease and schizophrenia reveals shared genetic architecture and identifies novel risk loci. Biol Psychiatry. 2021;89(3):227–35.
27. Buniello A, MacArthur JAL, Cerezo M, Harris LW, Hayhurst J, Malangone C, McMahon A, Morales J, Mountjoy E, Sollis E, et al. The NHGRI-EBI GWAS catalog of published genome-wide association studies, targeted arrays and summary statistics 2019. Nucleic Acids Res. 2019;47(D1):D1005–12.
28. Wang K, Li M, Hakonarson H. ANNOVAR: functional annotation of genetic variants from high-throughput sequencing data. Nucleic Acids Res. 2010;38(16):e164.
29. Kircher M, Witten DM, Jain P, O'Roak BJ, Cooper GM, Shendure J. A general framework for estimating the relative pathogenicity of human genetic variants. Nat Genet. 2014;46(3):310–5.
30. Boyle AP, Hong EL, Hariharan M, Cheng Y, Schaub MA, Kasowski M, Karczewski KJ, Park J, Hitz BC, Weng S, et al. Annotation of functional variation in personal genomes using RegulomeDB. Genome Res. 2012;22(9):1790–7.
31. Kundaje A, Meuleman W, Ernst J, Bilenky M, Yen A, Heravi-Moussavi A, Kheradpour P, Zhang Z, Wang J, Ziller MJ, et al. Integrative analysis of 111 reference human epigenomes. Nature. 2015;518(7539):317–30.
32. Ashburner M, Ball CA, Blake JA, Botstein D, Butler H, Cherry JM, Davis AP, Dolinski K, Dwight SS, Eppig JT, et al. Gene ontology: tool for the unification of biology. The gene ontology consortium. Nat Genet. 2000;25(1):25–9.
33. Aguet F, Brown AA, Castel SE, Davis JR, He Y, Jo B, Mohammadi P, Park Y, Parsana P, Segrè AV, et al. Genetic effects on gene expression across human tissues. Nature. 2017;550(7675):204–13.
34. Smith GD, Ebrahim S. Mendelian randomization': can genetic epidemiology contribute to Understanding environmental determinants of disease? Int J Epidemiol. 2003;32(1):1–22.
35. Burgess S, Davies NM, Thompson SG. Bias due to participant overlap in two-sample Mendelian randomization. Genet Epidemiol. 2016;40(7):597–608.
36. Burgess S, Butterworth A, Thompson SG. Mendelian randomization analysis with multiple genetic variants using summarized data. Genet Epidemiol. 2013;37(7):658–65.
37. Bowden J, Davey Smith G, Burgess S. Mendelian randomization with invalid instruments: effect Estimation and bias detection through Egger regression. Int J Epidemiol. 2015;44(2):512–25.
38. Bowden J, Davey Smith G, Haycock PC, Burgess S. Consistent Estimation in Mendelian randomization with some invalid instruments using a weighted median estimator. Genet Epidemiol. 2016;40(4):304–14.

39. Hartwig FP, Davey Smith G, Bowden J. Robust inference in summary data Mendelian randomization via the zero modal Pleiotropy assumption. Int J Epidemiol. 2017;46(6):1985–98.
40. Verbanck M, Chen CY, Neale B, Do R. Detection of widespread horizontal Pleiotropy in causal relationships inferred from Mendelian randomization between complex traits and diseases. Nat Genet. 2018;50(5):693–8.
41. Hemani G, Zheng J, Elsworth B, Wade KH, Haberland V, Baird D, Laurin C, Burgess S, Bowden J, Langdon R et al. The MR-Base platform supports systematic causal inference across the human phenome. Elife 2018, 7.
42. Ahangari M, Everest E, Nguyen TH, Verrelli BC, Webb BT, Bacanu SA, Tahir Turanli E, Riley BP. Genome-wide analysis of schizophrenia and multiple sclerosis identifies shared genomic loci with mixed direction of effects. Brain Behav Immun. 2022;104:183–90.
43. Anwar S, Shamsi A, Kar RK, Queen A, Islam A, Ahmad F, Hassan MI. Structural and biochemical investigation of MARK4 inhibitory potential of cholic acid: towards therapeutic implications in neurodegenerative diseases. Int J Biol Macromol. 2020;161:596–604.
44. Ahrari S, Mogharrab N, Navapour L. Structure and dynamics of inactive and active MARK4: conformational switching through the activation process. J Biomol Struct Dyn. 2020;38(8):2468–81.
45. Visscher PM, Wray NR, Zhang Q, Sklar P, McCarthy MI, Brown MA, Yang J. 10 Years of GWAS discovery: biology, function, and translation. Am J Hum Genet. 2017;101(1):5–22.
46. Hatipoglu E, Gunaldi O, Erkan B, Avcikurt A, Mert M, Niyazoglu M. Ubiquitin-specific protease 8 gene expression in sporadic pituitary adenomas. Neuro Endocrinol Lett. 2022;43(2):129–33.
47. Ma ZY, Song ZJ, Chen JH, Wang YF, Li SQ, Zhou LF, Mao Y, Li YM, Hu RG, Zhang ZY, et al. Recurrent gain-of-function USP8 mutations in Cushing's disease. Cell Res. 2015;25(3):306–17.
48. Dos Santos RS, Marroqui L, Velayos T, Olazagoitia-Garmendia A, Jauregi-Miguel A, Castellanos-Rubio A, Eizirik DL, Castaño L, Santin I. DEXI, a candidate gene for type 1 diabetes, modulates rat and human pancreatic beta cell inflammation via regulation of the type I IFN/STAT signalling pathway. Diabetologia. 2019;62(3):459–72.
49. Demenais F, Margaritte-Jeannin P, Barnes KC, Cookson WOC, Altmüller J, Ang W, Barr RG, Beaty TH, Becker AB, Beilby J, et al. Multiancestry association study identifies new asthma risk loci that colocalize with immune-cell enhancer marks. Nat Genet. 2018;50(1):42–53.
50. Serrano-Pozo A, Das S, Hyman BT. APOE and Alzheimer's disease: advances in genetics, pathophysiology, and therapeutic approaches. Lancet Neurol. 2021;20(1):68–80.
51. Takata Y, Kikukawa M, Hanyu H, Koyama S, Shimizu S, Umahara T, Sakurai H, Iwamoto T, Ohyashiki K, Ohyashiki JH. Association between ApoE phenotypes and telomere erosion in Alzheimer's disease. J Gerontol Biol Sci Med Sci. 2012;67(4):330–5.
52. Fani L, Hilal S, Sedaghat S, Broer L, Licher S, Arp PP, van Meurs JBJ, Ikram MK, Ikram MA. Telomere length and the risk of Alzheimer's disease: the Rotterdam study. J Alzheimers Dis. 2020;73(2):707–14.

Publisher's note